



Building and Calibration of a FAST Model of the SWAY Prototype Floating Wind Turbine

Preprint

J.H. Koh

Nanyang Technological University Singapore

A. Robertson, J. Jonkman, and F. Driscoll

National Renewable Energy Laboratory

E.Y.K. Ng

Nanyang Technological University Singapore

*To be presented at the International Conference on Renewable
Energy Research and Applications (ICRERA)*

Madrid, Spain

October 20–23, 2013

**NREL is a national laboratory of the U.S. Department of Energy
Office of Energy Efficiency & Renewable Energy
Operated by the Alliance for Sustainable Energy, LLC.**

This report is available at no cost from the National Renewable Energy
Laboratory (NREL) at www.nrel.gov/publications.

Conference Paper

NREL/CP-5000-60096

September 2013

Contract No. DE-AC36-08GO28308

NOTICE

The submitted manuscript has been offered by an employee of the Alliance for Sustainable Energy, LLC (Alliance), a contractor of the US Government under Contract No. DE-AC36-08GO28308. Accordingly, the US Government and Alliance retain a nonexclusive royalty-free license to publish or reproduce the published form of this contribution, or allow others to do so, for US Government purposes.

This report was prepared as an account of work sponsored by an agency of the United States government. Neither the United States government nor any agency thereof, nor any of their employees, makes any warranty, express or implied, or assumes any legal liability or responsibility for the accuracy, completeness, or usefulness of any information, apparatus, product, or process disclosed, or represents that its use would not infringe privately owned rights. Reference herein to any specific commercial product, process, or service by trade name, trademark, manufacturer, or otherwise does not necessarily constitute or imply its endorsement, recommendation, or favoring by the United States government or any agency thereof. The views and opinions of authors expressed herein do not necessarily state or reflect those of the United States government or any agency thereof.

This report is available at no cost from the National Renewable Energy Laboratory (NREL) at www.nrel.gov/publications.

Available electronically at <http://www.osti.gov/bridge>

Available for a processing fee to U.S. Department of Energy and its contractors, in paper, from:

U.S. Department of Energy
Office of Scientific and Technical Information
P.O. Box 62
Oak Ridge, TN 37831-0062
phone: 865.576.8401
fax: 865.576.5728
email: <mailto:reports@adonis.osti.gov>

Available for sale to the public, in paper, from:

U.S. Department of Commerce
National Technical Information Service
5285 Port Royal Road
Springfield, VA 22161
phone: 800.553.6847
fax: 703.605.6900
email: orders@ntis.fedworld.gov
online ordering: <http://www.ntis.gov/help/ordermethods.aspx>

Cover Photos: (left to right) photo by Pat Corkery, NREL 16416, photo from SunEdison, NREL 17423, photo by Pat Corkery, NREL 16560, photo by Dennis Schroeder, NREL 17613, photo by Dean Armstrong, NREL 17436, photo by Pat Corkery, NREL 17721.



Printed on paper containing at least 50% wastepaper, including 10% post consumer waste.

BUILDING AND CALIBRATION OF A FAST MODEL OF THE SWAY PROTOTYPE FLOATING WIND TURBINE

Jian Hao Koh

Nanyang Technological University
Singapore

Jason Jonkman

National Renewable Energy Laboratory
Golden, Colorado, USA

Frederick Driscoll

National Renewable Energy Laboratory
Golden, Colorado, USA

Amy N. Robertson

National Renewable Energy Laboratory
Golden, Colorado, USA

Eddie Y. K. Ng

Nanyang Technological University
Singapore

Abstract—Present efforts to verify and validate aero-hydro-servo-elastic numerical simulation tools that predict the dynamic response of a floating offshore wind turbine are primarily limited to code-to-code comparisons or code-to-data comparisons using data from wind-wave basin tests. In partnership with SWAY AS, the National Renewable Energy Laboratory (NREL) installed scientific wind, wave, and motion measurement equipment on the 1/6.5th-scale prototype SWAY floating wind system to collect data to validate a FAST model of the SWAY design in an open-water condition. Nanyang Technological University (NTU), through a collaboration with NREL, assisted in this validation.

This paper shows the use of the results of the SWAY open-water tests to calibrate the numerical FAST model, which will be used for future validation efforts. First, the modeling strategies and development of the FAST model for the SWAY prototype wind turbine are presented, including justification of the modeling assumptions. Next, the model calibration—based on a subset of the free-decay test data—is shown. This process involved tuning properties of the FAST model where uncertainties existed to better match the response of the prototype wind turbine. Finally, limitations of the FAST model and potential areas of improvement of the project are discussed.

Keywords—offshore wind; FAST; aero-hydro-servo-elastic; open-water testing

I. INTRODUCTION

In the design process, it is essential to use accurate numerical simulation tools to predict the complex aero-hydro-servo-elastic response of a floating wind turbine. Numerical simulation tools, such as FAST, developed by the National Renewable Energy Laboratory (NREL) [1], [2] are capable of modeling floating wind turbines and predicting their dynamic response behavior.

Presently, efforts are primarily focused on verifying these tools through code-to-code comparisons (International Energy Agency (IEA) Wind Offshore Code Comparison Collaboration (OC3) [3] and OC3 Continuation (OC4) projects [4]) of simulated system behavior.

Few physical tests have been used to compare experimental results with simulation data for floating wind systems. Browning and Goupee [5], Stewart et al. [6], Prowell et al. [7], and Coulling

et al. [8] worked on the calibration and validation of a FAST model with wind-wave basin tests conducted at the Maritime Research Institute Netherlands (MARIN) led by the DeepCwind consortium. In this work, the measurements from a 1/50th-scale spar, tension-leg platform, and semisubmersible floating wind turbine were scaled up and compared with results from full-scale FAST models of similar systems. In these three studies, the responses compared well between the experiment and the simulation in the wave-excitation frequency range after model calibration. These studies also indicated that the inclusion of second-order hydrodynamics and a dynamic mooring line model improve the accuracy of the simulations.

Almost all published studies to date on code-to-data validation work use data generated from a laboratory setting. Calibration and validation using response and performance data from real environmental conditions is beneficial to the development of aero-hydro-servo-elastic numerical tools as such tests are performed in realistic environmental conditions. In addition, larger-than-laboratory-scale testing will yield results with less scaling issues as it is able to show the overall system characteristic behavior more accurately.

This paper will focus on the effort to use the open-water test data of the SWAY prototype wind turbine to calibrate a FAST floating offshore wind turbine model for future validation efforts. This is the first time that the FAST tool has been compared to a real floating wind turbine system deployed in open water, which has a number of challenges compared to tank testing.

II. FAST WIND TURBINE SIMULATION TOOL

The FAST software tool developed by NREL is capable of modeling the coupled aero-hydro-servo-elastic response of a floating wind turbine subjected to combined wind and wave loading in the time domain.

Aerodynamic loads are calculated in the AeroDyn module, which has the option of using blade element momentum (BEM) theory or a generalized dynamic wake theory with steady or unsteady airfoil aerodynamics, including dynamic stall. The user also has the option of including the effects of Prandtl's tip and hub losses [9].

Structural components of the wind turbine are modeled by a combined nonlinear multibody dynamics and modal superposition formulation. Structural components such as the blades, tower, and driveshaft can be modeled as flexible bodies, while the platform and nacelle are modeled as rigid bodies.

The HydroDyn module [2] computes the time-domain hydrodynamics loading based on nonlinear viscous drag from waves and current, the linear added mass and damping from wave radiation, and linear wave excitation including diffraction. A nonlinear, quasi-static mooring line model is also available for floating wind turbines to calculate loads from taut or catenary lines, including the effect of stretching, buoyancy, mass density, and seabed interactions.

The degrees of freedom (DOFs) of the floating wind turbine, as modeled in FAST, include tower bending, blade bending, nacelle/rotor yaw, generator azimuth, driveshaft torsion, and platform motion. The platform DOFs are translated in the X , Y , and Z directions and are called surge, sway, and heave; and rotations about the X , Y , and Z axes are called roll, pitch, and yaw. Each DOF can be turned on or off individually. Figure 1 shows the coordinate systems and platform DOF terminology used in this paper; the origin is located at the mean sea level (MSL) and dimensions described in this paper will be referenced to this inertial frame coordinate system unless otherwise stated.

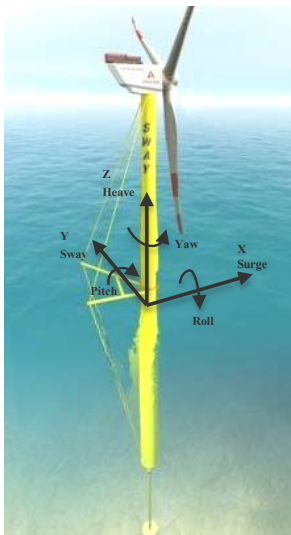


Figure 1. Coordinate systems and platform DOF.

III. SWAY SPAR-TYPE FLOATING WIND TURBINE

The SWAY spar-type floating wind turbine (Figure 2) has a three-bladed downwind configuration that uses a tension rod system for station-keeping and to maintain the hydrostatic stability of the wind turbine. The bottom of the spar structure is fixed to the tension rod with a universal joint. The other end of the tension rod is attached to a large steel mass (gravity anchor) on the seafloor with another universal joint. A downwind configuration allows the use of a passive yaw system that eliminates the cost that would be incurred by having an active yaw system in an upwind design. The wind turbine system, including the tower, yaws about the yaw mechanism located at the universal joint at the bottom of the tower. In addition, the

blade clearance from the tower, which is an issue for larger turbines, is less of a concern for the downwind SWAY turbine.

The wind turbine has individual blade-pitch control, and the nacelle is fixed to the tower at an optimal angle such that the rotor axis is oriented horizontally (parallel to the wind) when the tower pitches during operation. Some of the key components in the system include unique spreader beams and tension cables, which help to stiffen the tower, reduce fatigue loads, and allow the tower to carry a larger turbine.

The full-scale SWAY wind turbine is designed to have a rated power of 2.5–10 MW, a rotor diameter up to 124 m, and a support structure up to 210 m in length.

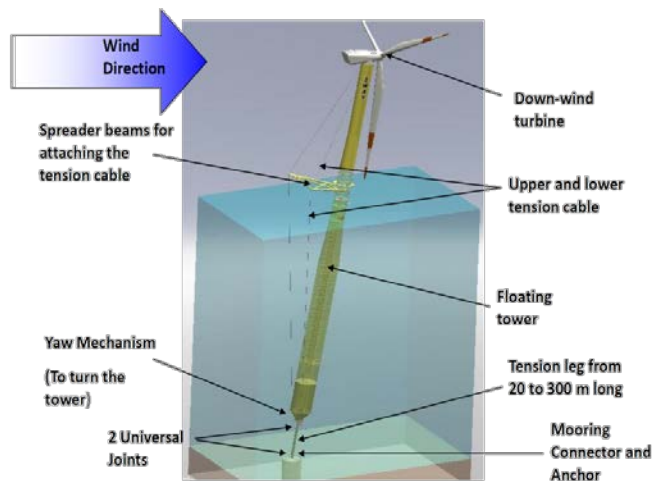


Figure 2. SWAY floating wind turbine.

A 1/6.5th-scale prototype of the SWAY spar-type floating wind turbine was deployed in Hjeltefjorden, east of Øygarden in Hordaland, Norway, in May 2012 (www.sway.no). As part of a collaboration between NREL and SWAY AS, NREL installed scientific wind, wave, and motion measurement equipment on the SWAY system. The equipment enhances SWAY's data collection and will allow SWAY to verify the concept and NREL to validate a model of the SWAY design in an open-water condition. NTU, in collaboration with NREL, is assisting with the validation.

Table 1 provides the key specifications of the prototype wind turbine. Other detailed specifications, such as system dimensions and blade and mass properties, are not shown in the report because of proprietary protections.

TABLE I. SWAY 1:6.5 SCALE WIND TURBINE PROTOTYPE SPECIFICATIONS

Foundation Manufacturer	SWAY
Make, Model of Turbine	SWAY1/6.5 th Scale Prototype
Production Year of Turbine	2011
Rotation Axis	Horizontal
Orientation	Downwind
Number of Blades	3
Rotor Diameter (m)	14.9
Hub Height (m)	~13
Control	Individual Pitch Control
Tower Type	Tubular
Floater Type	Spar Buoy

The platform motions were measured with two motion reference units (MRU). A Teledyne DMS-05 MRU was located in the tower near the centerline just above the waterline and an Xsens MTi-G motion tracker unit was located out on an anemometer boom at nacelle height. A dual antenna Hemisphere VT101 GPS was used to provide position and heading. The wind speed and direction were measured with two three-axis ATI SATI/3K ultrasonic anemometers. One was mounted upwind on the same boom as the MTi-G and the other was mounted near the base of the nacelle. Profiles of the water velocity and directional wave spectra were measured by a Nortek 600 kHz acoustic wave and current profiler (AWAC) mounted in an OceanScience Sea Spider subsea instrumentation tripod approximately 12 m north-northeast of the turbine at a depth of about 20 m.

Instruments aboard the turbine are sampled with a National Instruments PXI system located in the tower base. Data is stored both aboard the PXI system and transmitted to the shoreside computer. Data from the AWAC are internally recorded and loaded to a shoreside computer via an underwater communication cable. The PXI was chosen because of its ability to rapidly interrogate sensors that are widely distributed and its ability to use GPS time to tightly coordinate and synchronize measurements. This data acquisition system is monitored and controlled remotely at NREL in Golden, Colorado (USA).

Figure 3 shows the profile of the tower, spreader beam, and tension rod. In FAST, the blue region is modeled as the wind turbine tower while the red region is modeled as the platform. Yellow circles indicate the locations of the instruments.

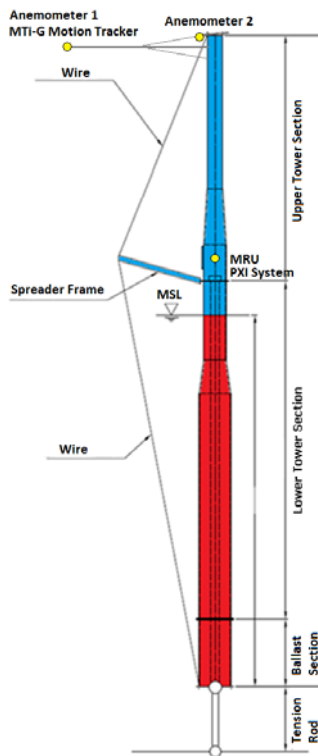


Figure 3. Profile of the tower, spreader beam, and tension rod.

IV. FAST MODEL

A FAST model of the system was created using the specifications of the SWAY 1/6.5th-scale prototype spar-type floating wind turbine. As such, the model and test data obtained do not require any form of scaling when compared, eliminating potential scaling errors.

A. Assumptions

The SWAY wind turbine includes some innovative components that cannot be modeled directly (without customization) in the existing FAST tool.

The tension wires and spreader-beam system generates an asymmetric stiffening of the tower in the fore and aft directions. However, the current version of FAST is only able to model symmetric properties for the tower. For this work, the tower-bending flexibility was considered to be negligible because the wind turbine is freely floating and no significant bending moments were applied at the bottom of the structure. As such, the tower was modeled as a rigid structure as a first step in getting a working model.

The yawing of the wind turbine occurs at the yaw mechanism, which is located at the bottom of the spar, as opposed to a conventional yaw bearing located at the nacelle. There is a reasonable amount of yaw damping that arises from aerodynamic drag, hydrodynamic drag, and friction forces at the two universal joints. But, as yaw motion is not of specific interest in the free-decay work discussed in this paper, the nacelle and platform yaw DOF were switched off to restrict any yaw motion of the wind turbine.

The SWAY turbine uses a tension rod instead of typical slack or taut mooring lines commonly used for floating offshore platforms. As described earlier, FAST has a quasi-static mooring line model. To represent the tension rod in the FAST model, it is modeled as a taut mooring line. This assumption is valid because the SWAY wind turbine should only generate tension forces under the design conditions. Therefore, thickness, mass, and stiffness properties of the tension rod were used for the mooring-line model.

V. MODEL CALIBRATION

For this study, most of the wind turbine dimensions and blade properties were provided by SWAY AS. However, there were some uncertainties in quantities, such as the mass moment of inertia and tower-mass distribution. Before the wind turbine was deployed, a center of gravity test was performed for the whole system. From the mass properties and center of gravity (CG) location data, the tower and platform properties were adjusted to match the CG location of the model with the real system. Because of the lack of measured data of the inertia values, they were the primary values used to calibrate the model to the experimental data. An additional quadratic global platform damping matrix was used to calibrate the model.

A. Static Equilibrium Comparison and Calibration

A FAST linearization analysis of the model was conducted under static-equilibrium conditions to check the full system characteristics. Full-system inertia, damping, and stiffness values were obtained to get a general understanding of the system and to verify the system properties.

A static-equilibrium simulation was initially carried out on an uncalibrated model to obtain the natural equilibrium position of the turbine. At equilibrium, the pitch offset (from upright position) was 1.8° and the surge offset was 0.514 m. The sway, heave, and roll offsets were negligible.

From experimental data, it was observed that the pitch offset is about 0.98° while the surge offset is about 0.34 m. To calibrate the offset, minor adjustments were made to the nacelle CG and the overhang values in FAST. This was a reasonable adjustment because of the inaccuracy in determining the mass distribution of the nacelle. After calibration, the pitch offset was 1° and the surge offset was 0.287 m.

B. Free-Decay Tests

Further calibration of the model was performed using free-decay test data. After turbine deployment and installation of the NREL instrumentation, five free-decay tests were conducted on the SWAY prototype by displacing the system and allowing it to return to equilibrium—two in the roll direction, and one each for the pitch, surge, and sway directions. Ropes were attached to the nacelle and the base of the tower to perform the displacement. The ropes were held with a quick release system and pulled onshore (nearby to the prototype installation) to set the system to the desired initial displacement of the system.

Testing was conducted during calm conditions with a mean wind speed of 1.7 m/s and minimum and maximum values of 0.25 m/s and 5 m/s, respectively. The ocean was predominately flat with very small wind-generated capillary waves. The current velocity ranged from 6 to 8 cm/s based on hourly averages. The turbine did not operate during the tests and it was expected that the calm conditions had minimal impact on the experimental data.

In an ideal condition, only one DOF would be excited at a time in a free-decay test to identify the frequency and damping of that DOF. However, during the actual test, the primary DOF of interest in each test was strongly coupled with other DOFs. For example, during a roll free-decay test, the sway DOF was heavily coupled while the pitch and surge of the system experienced small motions. Nonetheless, the results collected were sufficient to allow for manual tuning of the mass moment of inertia and drag coefficient (which results in hydrodynamic viscous damping) of the platform to calibrate the natural frequency and damping of the system.

Out of five free-decay tests, only one roll free-decay test and one pitch free-decay test were needed for calibration while the remaining tests will be used for validation in the future.

1) Roll Free-Decay Test

The initial displacements (surge, sway, and heave) and rotations (roll and pitch) from the roll free-decay test were used

as initial conditions in the FAST model. A free-decay simulation was then run, and the platform inertia and roll term (diagonal-only) in the damping matrix was tuned so that the roll period and magnitude matched the experimental data.

a) Roll DOF

The experiment exhibited an average platform roll period of 45.6 s. Although, the FAST simulation had an average period of 44.0 s after calibration. It is noted that both the experimental and simulated period varied slightly throughout the entire free-decay test (the first experimental oscillation period was 42.9 s). The roll motion of the system after tuning is shown in Figure 4. The simulated motion follows the experimental motion quite closely. Significant deviations of the period and amplitude occur after the fourth oscillation when the magnitude of oscillation decreases.

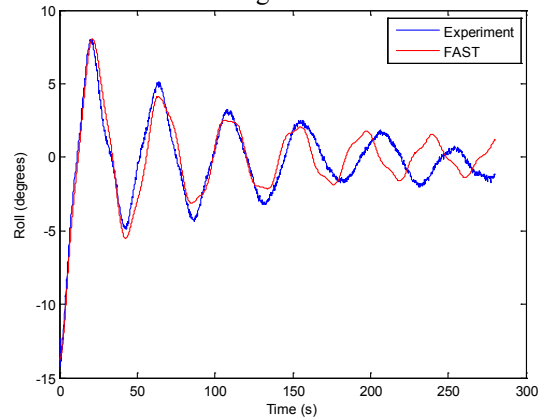


Figure 4. Roll motion in roll free decay.

A fast Fourier transform (FFT) was carried out for the first 280 s of experimental time and 5,000 s of simulation time to analyze the data in the frequency domain. Whereas the large amount of data for over 5,000 s of simulation time provided a decrease in power-spectral density across all frequencies, the peak frequencies became more pronounced, which is useful for improving the analysis and resolution of the FAST results. Figure 5 shows the FFT results, while Figure 6 zooms in around the main peaks. The peak frequency of the experimental and simulated results occurs at values of about 0.02143 Hz and 0.023 Hz, which correspond to a period of 46.7 s and 43.48 s, respectively. This is the roll frequency of the whole system.

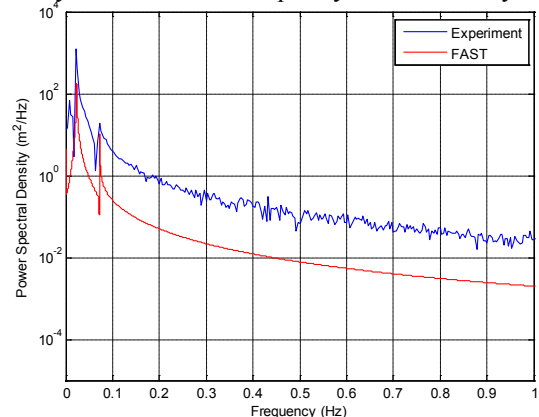


Figure 5. Power spectral density (PSD) versus frequency of roll DOF.

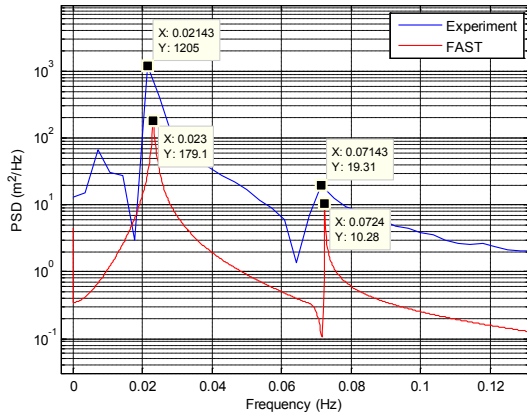


Figure 6. PSD versus frequency of roll DOF (zoomed in).

Because of the short duration of the roll test and sample rate, the range and resolution of the frequency data is limited at lower frequencies. For example, the next frequency higher than 0.02143 Hz is 0.025 Hz, whereby the period would have decreased to 40.0 s. Nonetheless, the FFT analysis shows matching frequency trends between experimental and simulation results.

A second peak frequency was also observed for simulated and experimental results occurring at values of about 0.0724 Hz and 0.07143 Hz, respectively. The second peak frequency is caused by the flexibility of the universal joint between the spar structure and tension rod, which allows both to rotate about this joint. This is verified by analyzing the measured angle of the tension rod with a motion plot and FFT analysis.

Figure 7 shows that the primary frequency of motion of the tension rod is higher compared to the rolling motion of the system in Figure 4. Figure 8 and 9 shows the FFT results, indicating that the primary frequency is 0.0681 Hz and 0.07168 Hz from the experimental data and FAST analysis respectively, which corresponds closely to the second peak shown in the FFT results in Figure 6.

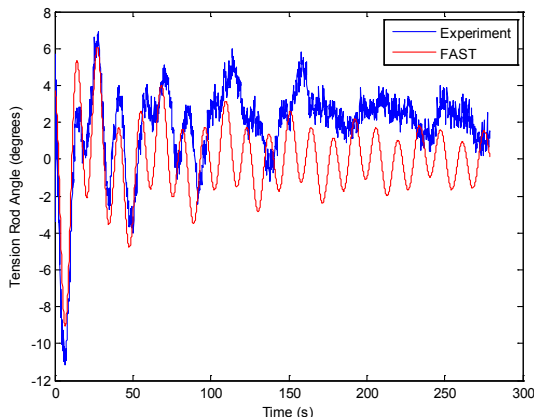


Figure 7. Tension rod motion.

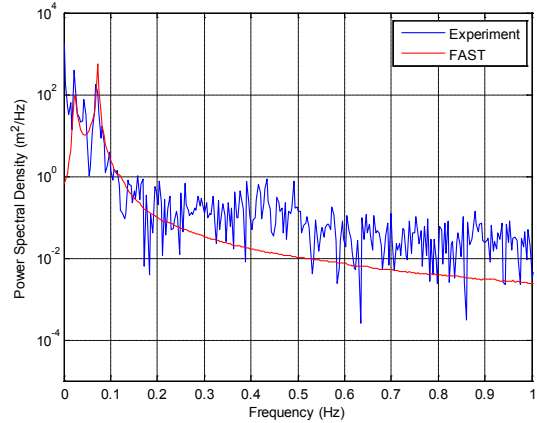


Figure 8. PSD versus frequency of tension rod motion.

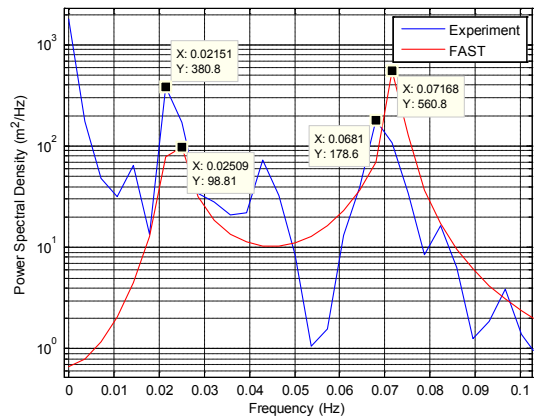


Figure 9. PSD versus frequency of tension rod motion (zoomed in).

2) Pitch Free-Decay Test

Next, initial displacements and rotations were set in the FAST model to match the starting conditions for the pitch free-decay test. The simulated response in FAST was used to tune the platform inertia and damping matrix in the pitch direction (diagonal-term) so that the pitch period matched that of the experimental data.

a) Pitch DOF

The experiment had an average platform pitch period of 44.6 s. After calibration, the FAST simulation had an average period of 42.9 s. Similarly, both the experimental and simulated period varied slightly throughout the entire free-decay test. For the first oscillation, the experimental period of the pitch motion was 42.5 s while the simulation period was 43.7 s. The pitch offset was similar (at about 1°) for the experimental and simulation results. The motion plots are shown in Figure 10. The simulated motion follows the experimental motion quite closely. Noticeable deviations for period and amplitude occur after the fifth oscillation when the magnitude of oscillation has decreased over time.

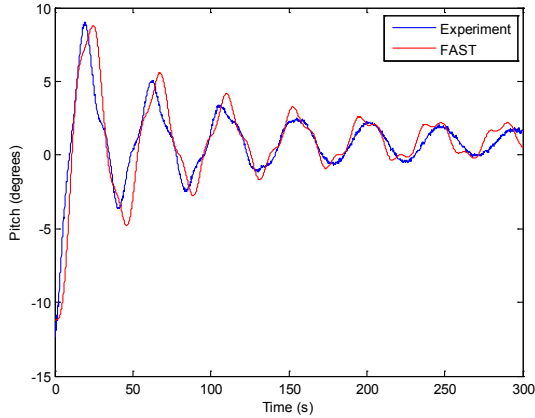


Figure 10. Pitch motion in pitch free decay.

An FFT was carried out for the first 300 s of experimental time and 5000 s of simulation time. Figure 11 shows the FFT results, while Figure 12 is zoomed in to show the peak values. The peak frequency of the measured and simulated pitch occurs at values of about 0.02333 Hz and 0.0226 Hz, which corresponds to a period of 42.86 s and 44.25 s, respectively. This frequency is the pitch frequency of the whole system. A second peak frequency is also observed for measured and simulated pitch occurring at values of about 0.07333 Hz and 0.0714 Hz. Similar to the roll free-decay analysis, the second peak frequency is caused by the flexibility of the universal joint between the spar structure and tension rod.

Because of the duration of the pitch test and sample rate, the range and resolution of the frequency data is limited at 0.00333 Hz. This error is significant at lower frequencies. For example, at the next frequency higher than 0.02333 Hz is 0.02667 Hz, whereby the period would have decreased to 37.5 s. Nonetheless, the FFT analysis shows matching frequency trends between experimental and simulation results.

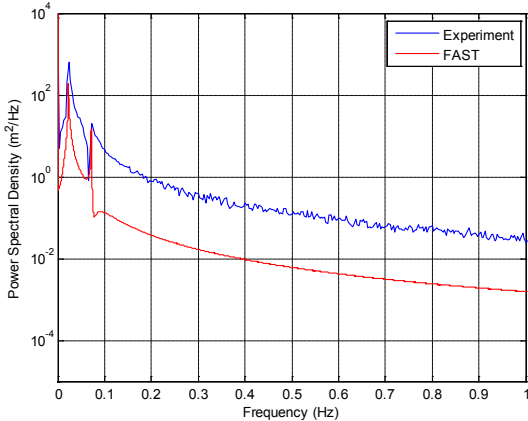


Figure 11. PSD versus frequency of pitch DOF.

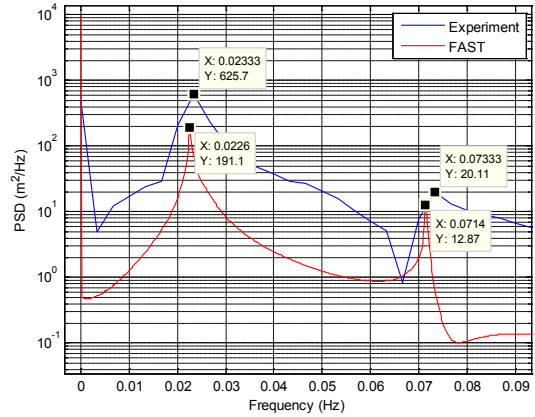


Figure 12. PSD versus frequency of pitch DOF (zoomed in).

The assumptions indicated earlier were likely to result in minor deviations between simulation and experimental results. In addition, there were two factors that might cause errors in period and amplitude as the magnitude of oscillation decreased over time.

The first factor is the inability to model frictional damping in the universal joints in the tension rod. During the initial few oscillations, the hydrodynamic viscous drag of the system is dominant. While the motion subsides overtime, the frictional damping in the universal joints may become significant in affecting the overall motion of the system.

The second factor was the inability to accurately simulate the drag coefficient of the cylindrical spar, which varies with the motion of the platform. This would likely result in minor errors for the simulated system.

In general, the calibrated FAST model was able to simulate the dynamics of the prototype SWAY wind turbine in free-decay motions with reasonable accuracy. However, to have better confidence in the model, more work needs to be done on the calibration process to reduce deviations in the simulated results and fine-tune the model over several periods. More data would help increase the confidence of the spectra.

VI. CONCLUSION

A FAST model of the SWAY prototype wind turbine was built and calibrated using two sets of free-decay tests. The comparison between the FAST simulations and experiment results matched with minor discrepancies because of the simplifying assumptions made in modeling the turbine. The inability to model frictional damping in the universal joints of the system and the inability to simulate the disturbed fluid field around the platform also contributed to discrepancies between measured and simulated results. Further work using more data sets and improved physics is needed to have a more accurate and reliable FAST model.

Future work may look at quantifying the assumptions and estimating the resulting errors. Also, the model fidelity may be increased to reduce assumptions. Some changes to the FAST tool might include altering the mooring-line model to better represent the tension-rod system and modifying the tower-stiffness model

to account for the spreader beam system, which is unique for the SWAY system. In addition, simulations of different turbine operating and nonoperating conditions will be conducted and validated to further the accuracy of the model and FAST's ability to model floating wind turbines.

ACKNOWLEDGMENT

The authors gratefully acknowledge the support provided by the U.S. Department of Energy and the Energy Research Institute at Nanyang Technological University. In addition, the expertise and support of SWAY AS in conducting the model test and providing valuable test data is greatly appreciated.

REFERENCES

- [1] J. Jonkman and M. L. B. Jr, "FAST User's Guide," 2005.
- [2] J. Jonkman, "Dynamics Modeling and Loads Analysis of an Offshore Floating Wind Turbine," Ph.D. dissertation, University of Colorado, United States, 2007.
- [3] J. Jonkman and W. Musial, "Offshore Code Comparison Collaboration (OC3) for IEA Task 23 Offshore Wind Technology and Deployment," United States, Rep, 2010.
- [4] W. Popko, F. Vorpahl, and A. Zuga, "Offshore Code Comparison Collaboration Continuation (OC4), Phase I Results of Coupled Simulations of an Offshore Wind Turbine with Jacket Support Structure," in 22nd International Society of Offshore and Polar Engineers Conference, Rhodes, Greece, 2012.
- [5] J. R. Browning and A. J. Goupee, "Calibration and Validation of a Spar-Type Floating Offshore Wind Turbine Model using the FAST Dynamic Simulation Tool Preprint," in Science of Making Torque from Wind, Oldenburg, Germany, 2012.
- [6] G. Stewart, M. Lackner, and A. Goupee, "Calibration and Validation of a FAST Floating Wind Turbine Model of the DeepCwind Scaled Tension-Leg Platform Preprint," in 22nd International Society of Offshore and Polar Engineers Conference, Rhodes, Greece, 2012.
- [7] I. Prowell, G. M. Stewart, and A. J. Goupee, "Numerical Prediction of Experimentally Observed Behavior of a Scale Model of an Offshore Wind Turbine Supported by a Tension-Leg Platform Preprint," in 2013 Offshore Technology Conference, Houston, Texas, 2013.
- [8] A. J. Coulling, A. J. Goupee, A. N. Robertson, J. M. Jonkman, and H. J. Dagher, "Validation of a FAST semi-submersible floating wind turbine numerical model with DeepCwind test data," *Journal of Renewable and Sustainable Energy*, vol. 5, no. 2, p. 023116, 2013.
- [9] P. J. Moriarty and A. Hansen, "AeroDyn Theory Manual," 2005.